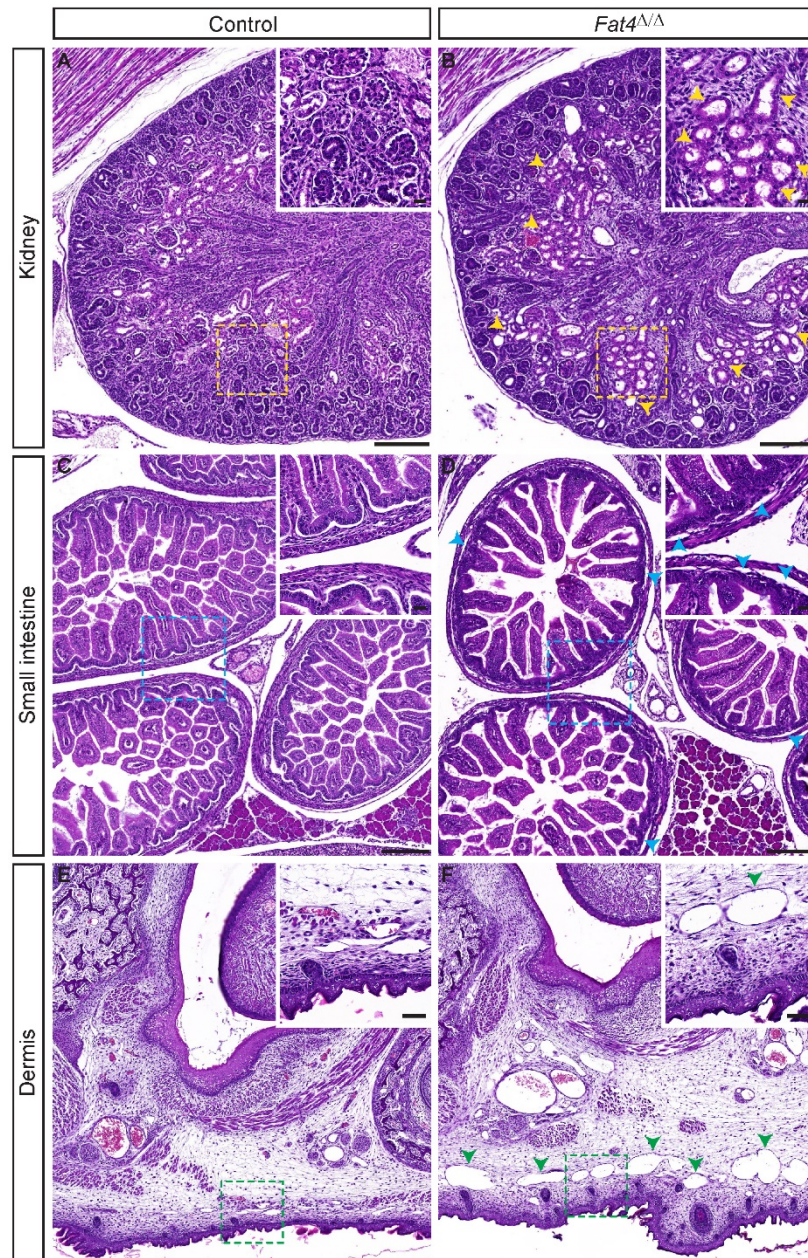


Supplemental Figure 1. The dermal blood vasculature is unaffected in *Fat4*^{Δ/Δ} embryos.

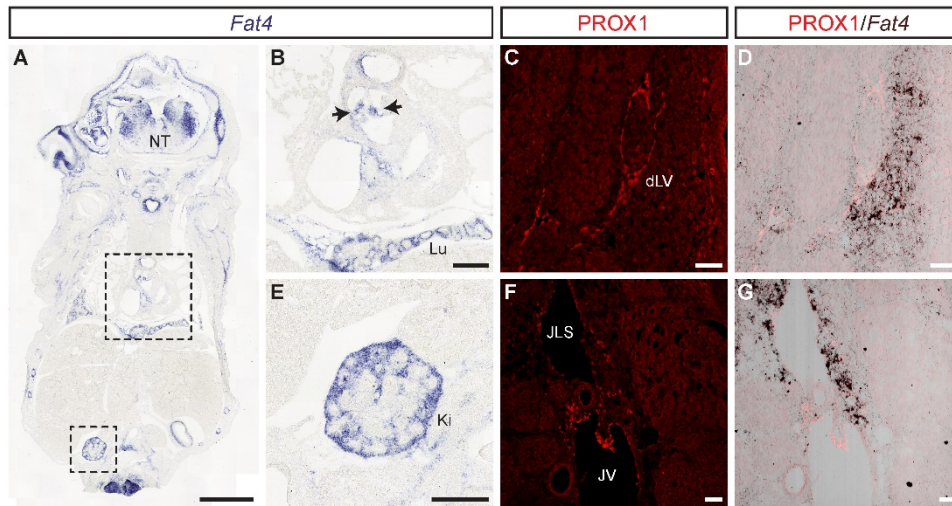
E14.5 dorsal skin montages stained with the pan-endothelial marker CD31 (green) revealed that patterning of the dermal blood vasculature is indistinguishable between control (A) and *Fat4*^{Δ/Δ} (B) embryos. Dashed line represents the dorsal midline. Scale bars: 100μm.



Supplemental Figure 2. *Fat4*^{Δ/Δ} embryos exhibit cystic kidney disease and lymphangiectasia.

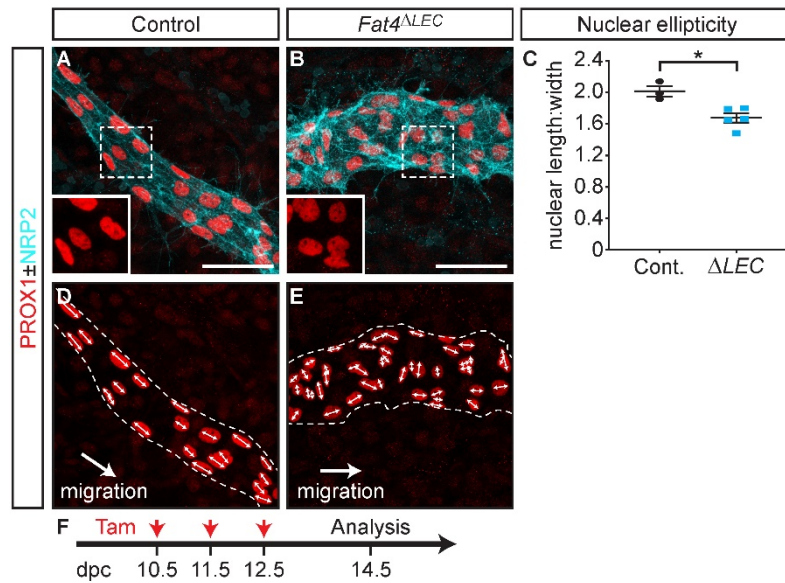
Histological analysis of H&E stained E18.5 control (A, C, E) and *Fat4*^{Δ/Δ} (B, D, F) embryonic tissue sections revealed that loss of *Fat4* results in multifocal tubular dilations in the kidney (yellow arrowheads, B), along with dilated submucosal (blue arrowheads, D) and dermal (green arrowheads, F) lymphatic vessels. Insets

represent higher magnification images of boxed regions. Scale bars: 200 μ m (**A** - **F**), 20 μ m (**A** - **D** insets) or 50 μ m (**E**, **F** insets).



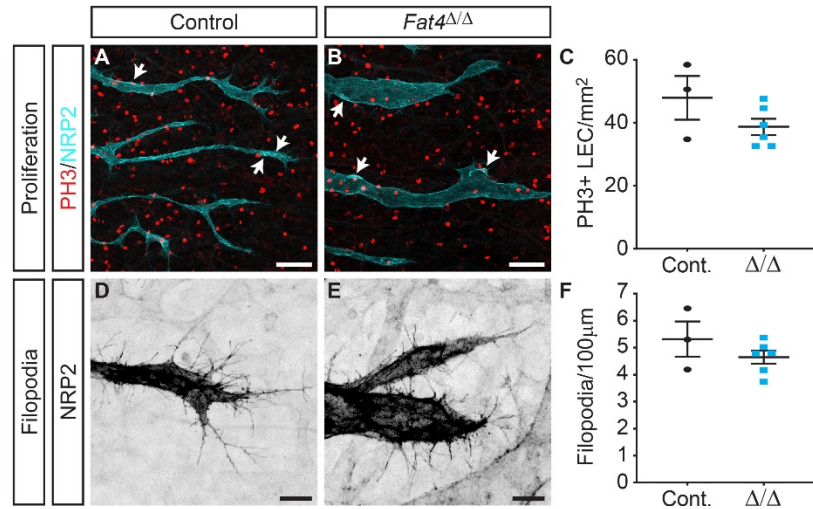
Supplemental Figure 3. *Fat4* mRNA is expressed in cardiac valves and the mesenchyme surrounding lymphatic vessels.

(A, B, E) RNA *in situ* hybridization of E14.5 coronal mouse tissue sections demonstrates prominent *Fat4* expression in the neural tube (NT), lung (Lu), kidney (Ki) and developing cardiac valves (black arrows, B). Co-staining with PROX1 (red) demonstrates that *Fat4* mRNA is also abundant in the mesenchyme surrounding dermal lymphatic vessels (dLV, C, D) and jugular lymph sacs (JLS, F, G), but not jugular veins (JV). C and F represent PROX1-only immunofluorescence channels corresponding to panels D and G, respectively. B and E depict higher magnifications of boxed regions in A. Scale bars: 1mm (A), 250µm (B, E) or 50µm (C, D, F, G).



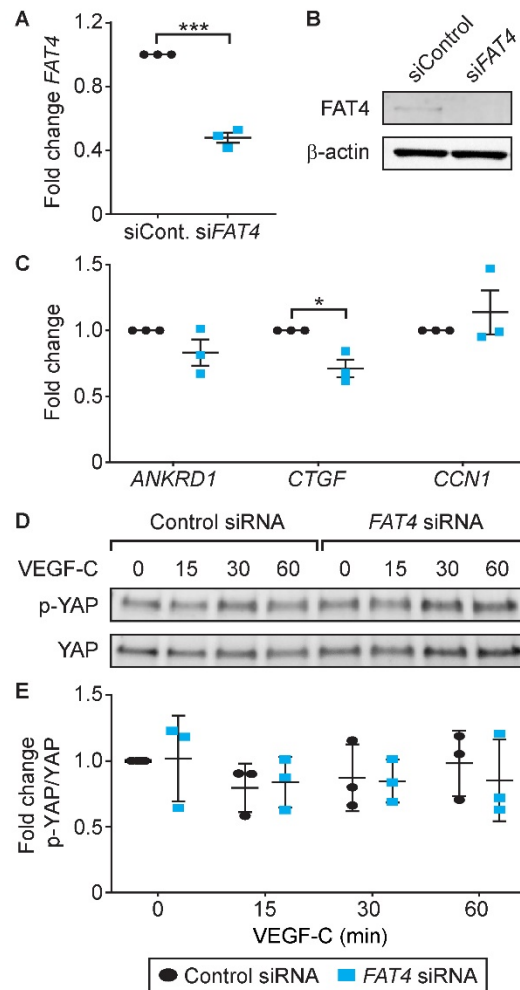
Supplemental Figure 4. Lymphatic endothelial cell polarity is impaired in *Fat4* ^{ΔLEC} embryos.

Prox1CreERT2;Fat4^{flax/flax} male mice were crossed with *Fat4^{flax/flax}* females and tamoxifen (20mg/ml, red arrows) was administered to pregnant females intraperitoneally at 10.5, 11.5 and 12.5 dpc (F). Whole mount immunostaining of the sprouting front in E14.5 dorsal skins stained for PROX1 (red) and NRP2 (cyan) revealed that *Fat4* ^{ΔLEC} LECs were more rounded (A - C) and exhibited reduced nuclear ellipticity (C) compared to littermate controls. Representative vessel schematics (D, E), based on A and B, respectively, highlight disorganized nuclear elongation axes (white double arrows) with respect to direction of vessel migration (white arrows) in *Fat4* ^{ΔLEC} embryos. Error bars correspond to \pm SEM, n = 3 control, 5 *Fat4* ^{ΔLEC} embryos (2 independent E14.5 litters). * P < 0.05 by 2-tailed Student's t test. Insets represent higher magnification images of boxed regions. Scale bars: 50 μ m.



Supplemental Figure 5. Proliferation and filopodia number are not altered in *Fat4*^{Δ/Δ} dermal lymphatic vessels.

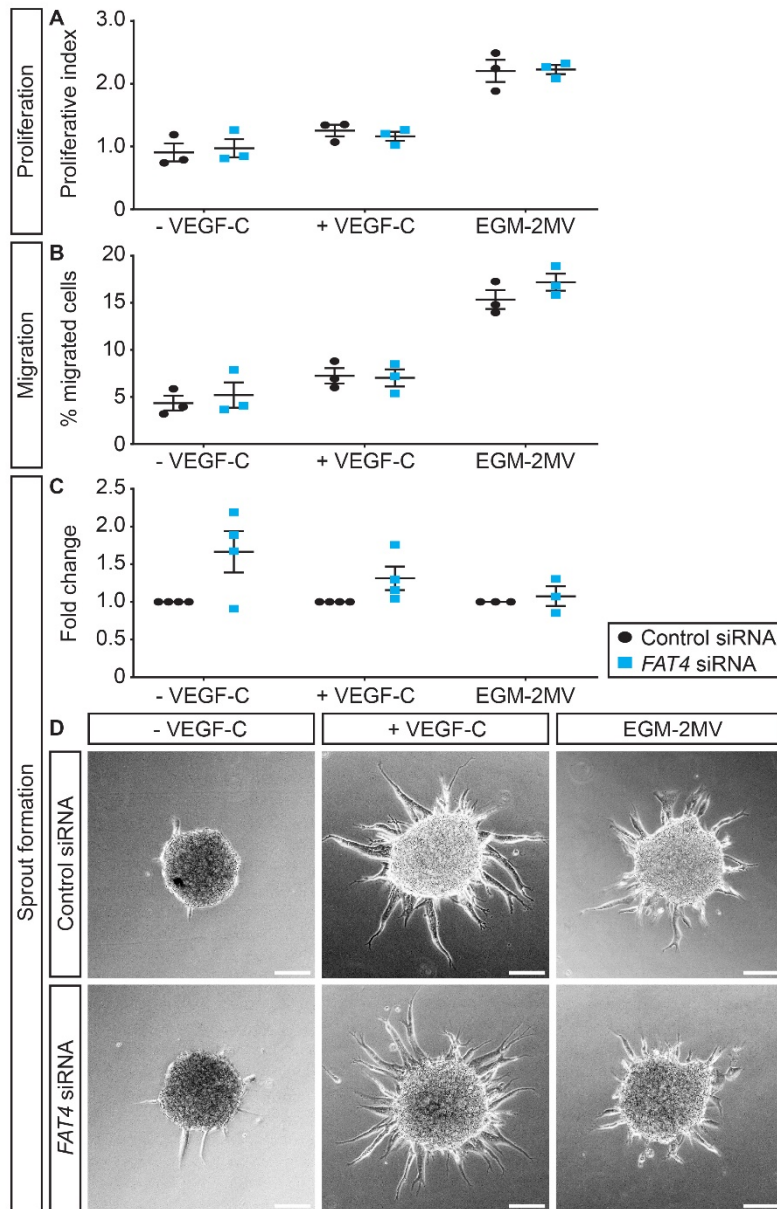
Whole mount immunostaining of E14.5 control (**A, D**) and *Fat4*^{Δ/Δ} (**B, E**) skins stained with phospho-histone H3 (PH3, red) to detect mitotic cells, and/or NRP2 to visualize the lymphatic vasculature and associated filopodia. Arrows illustrate PH3-positive proliferating dermal LECs. No difference in the number of PH3-positive LECs (normalized to vessel area (mm²), **C**), or the number of filopodia (normalized to 100μm vessel length, **F**) was observed between control and *Fat4*^{Δ/Δ} embryos. Error bars correspond to ± SEM, *n* = 3 control, 6 Δ/Δ embryos (3 independent litters). Scale bars: 100μm (**A, B**) or 25μm (**D, E**).



Supplemental Figure 6. Hippo pathway activity in *FAT4* deficient human lymphatic endothelial cells.

(A) *FAT4* mRNA is reduced ~55% in *FAT4* siRNA treated hLECs. Data represented as fold change in gene expression following normalization to *ALAS1*. (B) Representative Western blot probed with *FAT4* and β -actin (loading control) antibodies confirming efficient loss of *FAT4* protein in *FAT4* siRNA treated hLECs compared to control siRNA treated cells. (C) Expression of Hippo pathway target genes *ANKRD1*, *CTGF* and *CCN1* (CYR61) in *FAT4* siRNA treated hLECs compared to control cells. Data represented as fold change in gene expression following normalization to *ALAS1*. (D) Representative Western blots probed with antibodies detecting phospho-YAP and YAP following VEGF-C (100ng/ml) stimulation for 0,

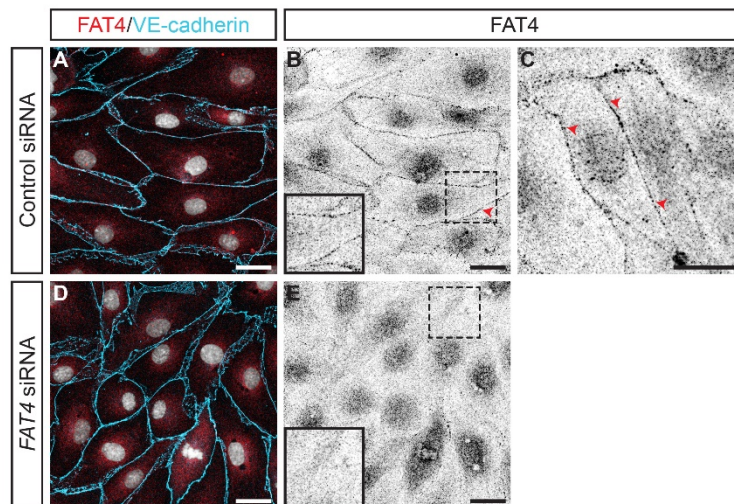
15, 30 and 60 minutes. **(E)** No differences in YAP phosphorylation were observed between control and *FAT4* siRNA treated hLECs following VEGF-C stimulation. Data represented as fold change in the ratio of phosphoYAP:YAP, relative to control treated cells at time 0. Error bars correspond to \pm SEM (**A, C**) or \pm SD (**E**), $n = 3$. * $P < 0.05$, *** $P < 0.0001$ by 2-tailed Student's t test.



Supplemental Figure 7. Proliferation, migration and sprouting of *FAT4* deficient human lymphatic endothelial cells in response to VEGF-C.

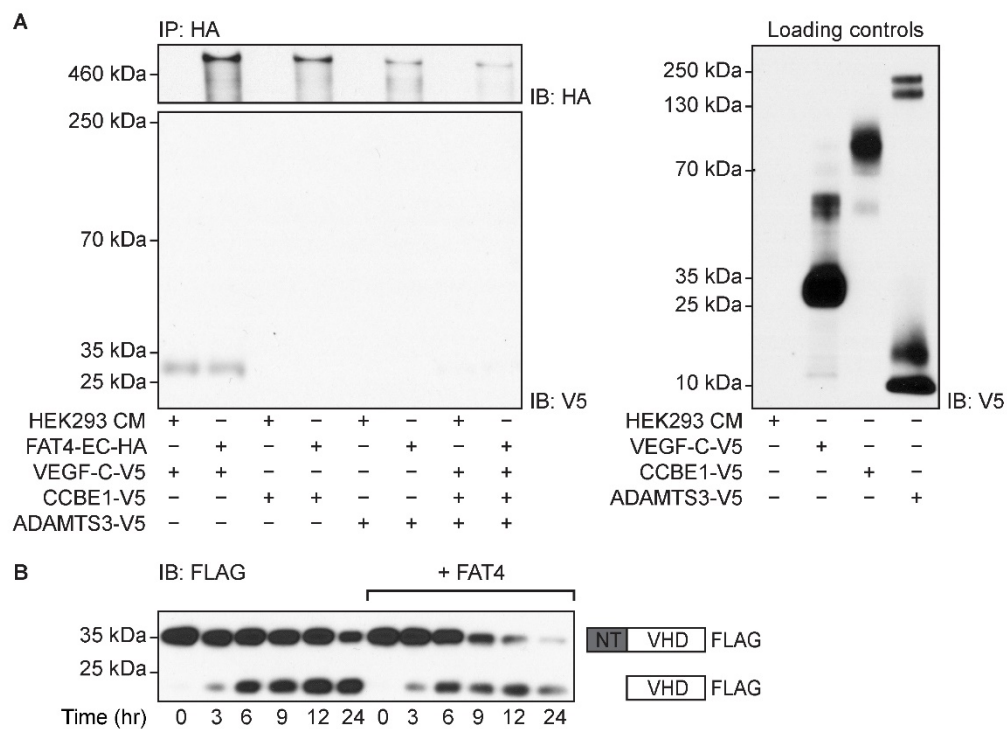
Proliferation (**A**), migration (**B**) and three-dimensional sprouting (**C**, **D**) of control and *FAT4* siRNA treated hLECs in response to basal media (EBM-2, 1% FBS - VEGF-C), basal media + VEGF-C (100ng/ml **A**, **B** or 200ng/ml **C**, **D**) or complete media (EGM-2MV). Data represented as proliferative index (cell number relative to initial number of cells plated, **A**), percentage of cells migrated relative to the number plated (**B**) or fold change in spheroid sprout formation relative to control

siRNA treated hLECs (**C**). (**D**) Representative spheroids formed from control and *FAT4* siRNA treated hLECs showing sprout formation after 24 hours. All experiments were performed in primary hLECs isolated from at least three independent donors. Error bars correspond to \pm SEM, $n = 3$ (**A**, **B**) or $n \geq 3$ (**C**). Scale bars: 100 μ m.



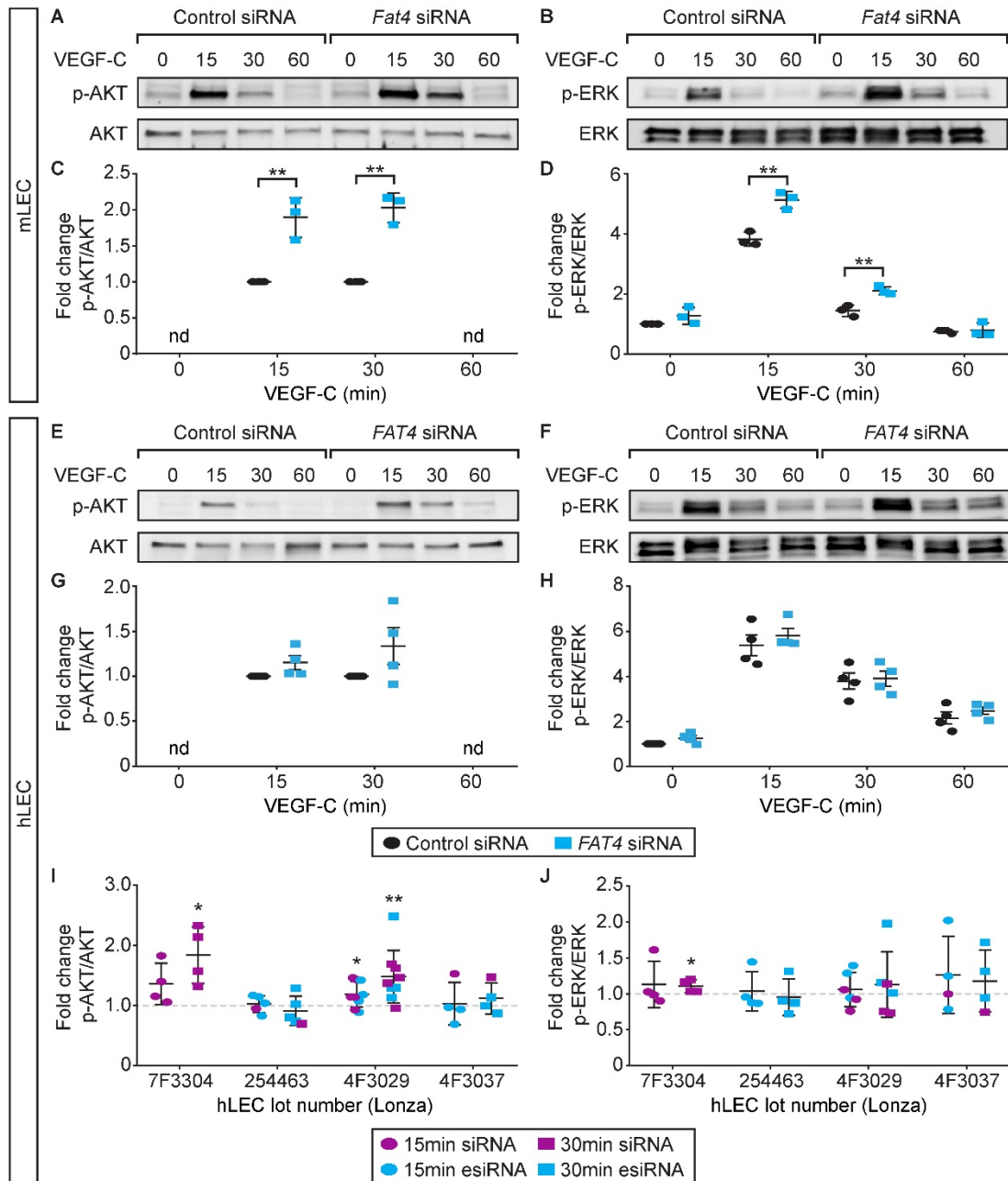
Supplemental Figure 8. FAT4 is localized at human lymphatic endothelial cell junctions.

FAT4 protein (red, **A, D** and black, **B, C, E**) is localized in a punctate pattern (arrowheads) at cell-cell junctions in cultured hLECs (**A - C**) and is absent in cells transfected with *FAT4* siRNA (**D, E**). VE-cadherin (cyan) and DAPI (white) demarcate the cell junctions and nuclei, respectively (**A, D**). Insets represent higher magnification images of boxed regions. Scale bars: 25μm.



Supplemental Figure 9. The extracellular domain of FAT4 does not promote CCBE1/ADAMTS3 mediated VEGF-C proteolysis.

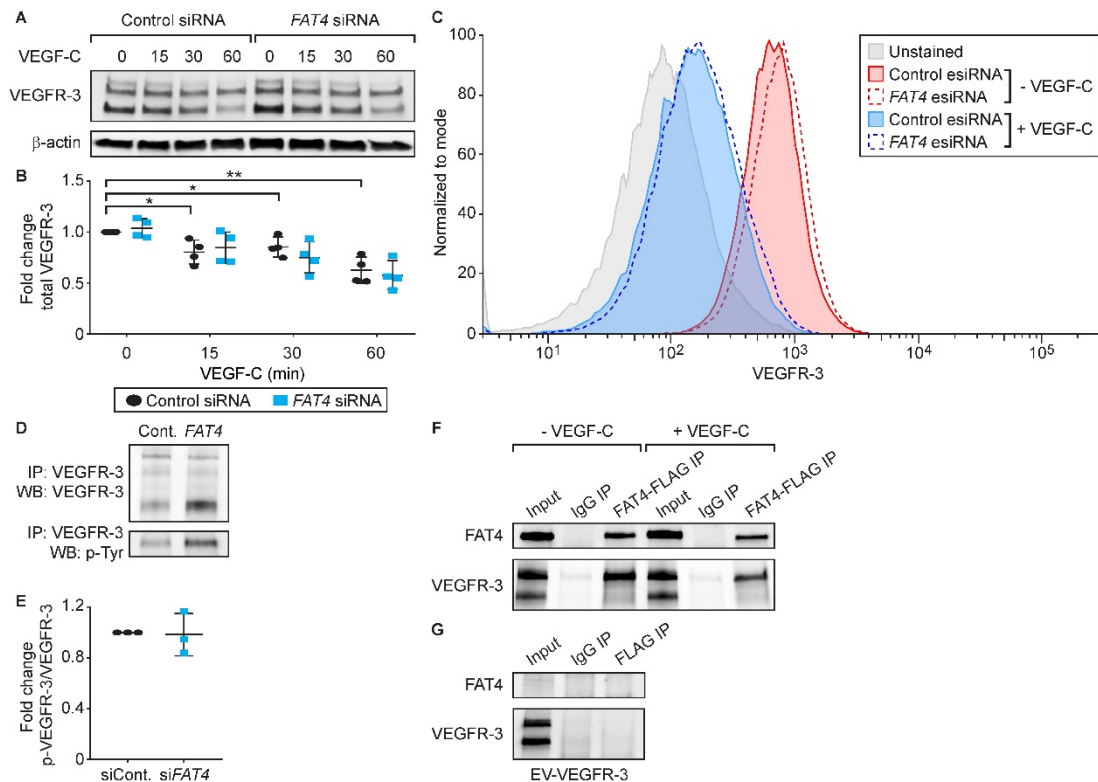
(A) Western blots probed with HA or V5 antibodies demonstrating that HA-tagged FAT4 extracellular domain does not co-immunoprecipitate with VEGF-C, CCBE1 or ADAMTS3. (B) The extracellular domain of FAT4 does not promote CCBE1/ADAMTS3 mediated proteolytic processing of VEGF-C in an in vitro assay.



Supplemental Figure 10. Response of *FAT4* deficient lymphatic endothelial cells to VEGF-C stimulation.

Representative Western blots probed with phospho-AKT and AKT (A, E) or phospho-ERK and ERK (B, F) antibodies following VEGF-C stimulation (200ng/ml for mLECs (A - D) or 100ng/ml for hLECs (E - J)). Elevated AKT (C, G) and ERK (D) activity in *FAT4* deficient cells compared to control cells following VEGF-C stimulation. Levels of AKT (C, G) activation represented as fold change in the ratio

of phospho/total protein relative to control treated cells. Levels of ERK (**D**, **H**) activation represented as fold change in the ratio of phospho/total protein relative to control treated cells at time 0. (**I**, **J**) Response of *FAT4* deficient hLECs from different donors to VEGF-C stimulation. AKT (**I**) and ERK (**J**) activity in *FAT4* deficient hLECs, transfected with either siRNA (purple) or esiRNA (blue), compared to control cells (represented as 1, grey dashed line) following VEGF-C stimulation for 15 (circles) or 30 (squares) minutes. Data represented as fold change in the ratio of phospho/total protein relative to control treated cells. Error bars correspond to \pm SD (**C**, **D**, **I**, **J**) or \pm SEM (**G**, **H**), $n = 3$ independent experiments using primary mLEC isolated from 17-24 embryos per experiment (**C**, **D**), $n = 4$ independent donor-derived batches of hLECs (**G**, **H**) or $n \geq 4$ for each batch of donor-derived hLECs (**I**, **J**). * $P < 0.05$, ** $P < 0.01$ by 2-tailed Student's t test. Nd: not determined.



Supplemental Figure 11. VEGFR3 levels and localization in *FAT4* deficient human lymphatic endothelial cells.

(A, B) Quantification of total VEGFR3 protein demonstrates levels of VEGFR3 are not significantly different between control and *FAT4* deficient hLECs pre- and post-VEGF-C stimulation. Data represented as fold change in total VEGFR3 relative to control at 0 minutes. (C) Cell surface levels of VEGFR3, assessed by flow cytometry, are similar between control and *FAT4* esiRNA treated hLECs \pm VEGF-C (100ng/ml for 15 minutes). Data shown is representative of three experiments. (D) Representative Western blots of immunoprecipitated VEGFR3 from control and *FAT4* siRNA treated hLECs probed with VEGFR3 and phospho-tyrosine (p-Tyr) antibodies following VEGF-C (100ng/ml) stimulation for 15 minutes. Consistently more VEGFR3 is immunoprecipitated from *FAT4* deficient cells. (E) Levels of VEGFR3 phosphorylation normalized to total VEGFR3 protein are similar between control and *FAT4* deficient hLECs. (F) Western blots probed with anti-FLAG-tag and anti-

VEGFR3 antibodies demonstrate that FLAG-tagged FAT4 intracellular domain co-immunoprecipitates with VEGFR3, independent of VEGF-C stimulation. **(G)** In the absence of FLAG-tagged FAT4 intracellular domain (EV, empty vector control), VEGFR3 co-immunoprecipitation was not observed. Error bars correspond to SD, $n = 4$ **(B)** or $n = 3$ **(E)**. * $P < 0.05$, ** $P < 0.01$ by 2-tailed Student's t test.

Primer	Primer sequence (5' - 3')
<i>ALAS1</i> forward	AGATCAAAGAAACCCCTCCG
<i>ALAS1</i> reverse	AGCTGTGTGCCATCTGGACT
<i>ANKRD1</i> forward	GTGTAGCACCAGATCCATCG
<i>ANKRD1</i> reverse	CGGTGAGACTGAACCGCTAT
<i>CCN1</i> forward	GCGTTTCCCTTCTACAGGCT
<i>CCN1</i> reverse	TCTCCAATCGTGGCTGCATT
<i>CTGF</i> forward	TGGAGATTTTGGGAGTACGG
<i>CTGF</i> reverse	CAGGCTAGAGAAGCAGAGCC
<i>DCHS1</i> forward	AGGAATAGGAGAGGAGGCCA
<i>DCHS1</i> reverse	CTACAATGCCTCACTGCCTG
<i>FAT4</i> forward	GTTCCAGTTCCAGTCAAGGC
<i>FAT4</i> reverse	TAACACAGAGTCTGGATCGGG

Supplemental Table 1. Primers used for investigation of mRNA levels in human lymphatic endothelial cells.